Research Square

Preprints are preliminary reports that have not undergone peer review.
They should not be considered conclusive, used to inform clinical practice,
or referenced by the media as validated information.

Three-Zone Radius Gradation and a Net Radiation Thrust Mechanism for Solar System Bodies

Zhao Dayong[1]

396804835@qq.com

Yueyang Civil Affairs Bureau

Wang Qijin[2]

Perspective

Keywords: exchange mechanics, net thrust formula, three-zone gradation, environmental exchange relation, origin of rotation, microscopic homology

Posted Date: November 16th, 2026

DOI: https://doi.org/10.21203/rs.3.rs-11421740/v1

License: This work is licensed under a Creative Commons Attribution 4.0 International License.
Read Full License

Additional Declarations: No competing interests reported.

Three-Zone Radius Gradation and a Net Radiation Thrust Mechanism for Solar System Bodies

Zhao Dayong[1],†, Wang Qijin[2]

[1] Yueyang Civil Affairs Bureau, Yueyang 414000, Hunan, China, 396804835@qq.com

[2] Hunan Nuclear Geology Survey Institute, Changsha 410000, China, 160877598@qq.com

† First author, corresponding author

Abstract:

Background: This Perspective article proposes, within the framework of exchange mechanics, a three-zone radius gradation pattern and a net radiation thrust mechanism for Solar System bodies, together with explicit falsification paths. Newtonian gravity and Kepler's laws reproduce planetary orbits, yet they do not explain the non-monotonic radius sequence, density stratification, or rotation differences of Solar System bodies from an intrinsic mechanism.

Methods: Using Solar System observations, we identify "three-zone gradation": body radius varies non-monotonically with heliocentric distance, peaking near Jupiter's and Earth's orbits. This empirical pattern motivates a hypothesis in which a body is a bipolar inlet–outlet structure—dayside absorbs solar radiation, nightside releases its own. From the first principle that electromagnetic waves carry momentum, we derive a net thrust formula, distinguishing a complete sphere (zero net force) from a hemisphere (non-zero).

Results: The formula (i) unifies bodies with and without significant internal heat; (ii) explains why thrust scales as R in the low-velocity zone; (iii) yields an environmental exchange relation $J \propto v_{\mathrm{rot}} \cdot \rho|_{\uparrow\downarrow}$, linking rapid giant-planet rotation (lowρ) to slow terrestrial-planet rotation (high ρ); and (iv) provides a consistent dynamical account of Kuiper Belt objects, Trojans, planetary rings, and cometary orbits.

Conclusions: The macroscopic architecture of the Solar System may include a net thrust from dayside–nightside radiation asymmetry. This effect may have been significant during the early planetesimal stage ($F_{\mathrm{net}}/F_{\mathrm{grav}} \sim 10^{-2} - 10^{0}$) but is only a minor modulation today ($F_{\mathrm{net}}/F_{\mathrm{grav}} \sim 10^{-15}$). Three-zone boundaries are empirical; their theoretical critical points require future numerical work.

Keywords: exchange mechanics; net thrust formula; three-zone gradation; environmental exchange relation; origin of rotation; microscopic homology

Statement of Paper Positioning

This Perspective article is a hypothesis paper, not a report of an established theory. The net thrust formula, the empirical pattern of three-zone gradation, and the environmental exchange relation proposed here are working hypotheses to be tested, not theories already supported by observations. The value of the paper lies in proposing a possible dynamical framework and in specifying clear falsification paths (Chapter 9). We welcome tests, criticism, and revision of these hypotheses by colleagues.

One point deserves particular emphasis. The quantitative effect of the thrust formula may have been significant during the early planetesimal stage ($F_{\mathrm{net}}/F_{\mathrm{grav}} \sim 10^{-2} - 10^{0}$), but it is only a minor modulation during the current planetary stage ($F_{\mathrm{net}}/F_{\mathrm{grav}} \sim 10^{-15}$). The discussions in Chapters 6 and 7 of the current planetary radius–density–rotation sequence should therefore be read as possible imprints left by thrust effects during the early stage, not as evidence that the present-day thrust directly determines planetary configuration.

Terminology. In this paper, "exchange flow" (J) refers collectively to the matter and energy exchanged through the inlet–outlet structure; our main focus is its electromagnetic radiation component. "Element–environment relation" denotes the theoretical relation $J \propto \rho$. "Element macroscopic distribution law" denotes the observational regularity that supports this relation, namely the element distribution in interstellar molecules. The two stand in a theory–evidence relationship.

1 Introduction

1.1 The problem

Newtonian gravity and Kepler's laws calculate planetary orbits with remarkable precision [1], and general relativity accounts for Mercury's perihelion precession [19]. Yet these frameworks do not explain, from an intrinsic mechanism, why Solar System bodies are distributed as they are. Three features of the macroscopic architecture remain without a unified dynamical account.

Orbital distribution. Mercury—the least massive planet ($0.055\ M_{\oplus}$)—occupies the innermost, fastest orbit (47.89 km/s), while Jupiter—the most massive ($317.83\ M_{\oplus}$)—sits at an intermediate distance ($13.06 km/s$) [2]. If gravity alone set orbital positions, one would expect some monotonic relation between mass and orbit. Observations show none.

Radius–density sequence. Planetary radius and mean density vary non-monotonically with heliocentric distance. From the outer planets to Earth, both radius and density increase; from Earth to Mercury, radius decreases while density stays high [2]. Density rises from Jupiter's 1.33 g/cm³ to Earth's 5.52 g/cm³, then remains near 5.46 g/cm³ at Mercury. The standard explanation—a formation-time temperature gradient—lacks a quantitative dynamical model.

Rotation. Classical mechanics treats rotation and revolution as kinematically independent and attributes rotation to primordial angular momentum. This does not explain why giant planets rotate rapidly in low-density space (Jupiter: 9.86 h) while terrestrial planets rotate slowly in high-density space (Earth: 23.93 h) [2].

These three problems point to one question: does the Solar System's architecture contain a dynamical component we have not yet recognized?

1.2 The gap

The three problems share two features.

They are **systematic:** parameters vary continuously along heliocentric distance, not randomly. This suggests a unified mechanism rather than independent accidents.

They show **trend reversal:** the radius gradation reverses near Jupiter's and Earth's orbits. The mechanism may act differently in different regions.

Existing models do not address this. The Nice model [3] and Grand Tack model [4] explain how planets reached their current orbits and how small bodies are distributed. Planet formation theory [5,6] explains accretion and compositional differentiation. None explains why bodies at these positions show the observed radius–density–rotation sequence. Specifically, existing models cannot answer: why radius is non-monotonic (increasing to Jupiter, decreasing to Mercury); why density rises monotonically from Jupiter to Earth but flattens from Earth to Mercury; or why rotation correlates systematically with mass rather than scattering randomly.

Building on the previously established matter–energy exchange framework [7,8,9,10], we extend the concept to the planetary system. In that framework, a body absorbs matter–energy through inlets and releases it through outlets, maintaining a steady state [9]. Earlier work [10] explored Solar System geological transitions from inlet–outlet structural forces, providing a basis for the thrust formula developed here.

1.3 Approach

We take a phenomenon-to-mechanism route.

Observation. From the largest representative bodies in different Solar System regions, we identify an empirical pattern: body radius peaks near Jupiter's orbit (about 5.2 AU) and Earth's orbit (about 1 AU). This summarizes observations; it is not derived from theory.

Hypothesis. To explain the pattern, we propose that radiation asymmetry between dayside and nightside hemispheres produces a net thrust.

The three-zone division is the empirical basis that motivated the formula, not a corollary of it.

1.4 Thrust source and distinction from existing mechanisms

1.4.1 Existing radiation pressure

Solar radiation pressure, $F_{\text{rad}} = \pi R^2 F_{\odot}(1-A)/c$, is negligible for planets. For Earth it is about $10^9 N$, against a gravitational force of $3.5 \times 10^{22} N$ ($F_{\text{rad}}/F_{\text{grav}} \approx 3 \times 10^{-14}$). The Yarkovsky effect scales as $\propto R3$ and is negligible at planetary scales [11].

1.4.2 Thrust from dayside–nightside asymmetry

The thrust here comes from the body's own radiation geometry. The dayside hemisphere absorbs solar radiation and produces a recoil away from the Sun. The nightside hemisphere releases its own radiation and produces a recoil toward the Sun. These are recoil forces; they superpose with gravity. F_{net} does not drive radial migration—it modulates the radial equilibrium position. Gravity determines roughly where a body sits; F_{net} determines where it settles.

Mechanism	Source	Direction	Scaling
Solar radiation pressure	Solar photon momentum	Away from Sun	$\propto R^2$
Yarkovsky	Body's anisotropic thermal radiation	Transverse	$\propto R^3$
This thrust	Dayside–nightside radiation difference	Radial	$\propto R^2$

What is new here: the thrust comes from hemisphere-vs-hemisphere asymmetry of the body's own radiation, not from external radiation or surface anisotropy.

1.5 Framework

The framework is called exchange mechanics; its core is inlet–outlet structure theory.

We introduce three elements.

Inlet–outlet structure (ontological assumption). A body is an open thermodynamic system. It absorbs matter–energy through an inlet, releases through an outlet, and maintains a steady state. The exchanged content is the exchange flow J. This paper focuses on its electromagnetic radiation component.

Element–environment relation (working hypothesis). An element's exchange quantity correlates positively with the density of the environment most suitable for it ($J \propto \rho$, symbolic). The basis is the statistical regularity of interstellar molecular element distribution (Section 4.1).

Net thrust formula (phenomenological model). Net thrust equals the difference between dayside and nightside radiation forces, derived from electromagnetic momentum flux.

The three form a progression: assumption, hypothesis, model.

"Celestial body" refers broadly to all Solar System objects. "Planet" refers to the eight planets.

1.6 Contributions

We establish a net thrust formula, distinguish sphere from hemisphere, and argue for the microscopic homology of electromagnetic radiation. We describe three-zone gradation and propose a mechanism. We propose $J \propto v_{\text{rot}} \cdot \rho$ (symbolic), where J is the product of rotation velocity and environmental density; when J is fixed, the two vary inversely. We give a consistent account of Kuiper Belt objects, the main asteroid belt, Trojans, planetary rings, and cometary orbits.

2 Three Velocity Zones of the Solar System and Implications of the Gradation Pattern

Using observational data for the eight planets and other bodies (Table 2), we divide the Solar System into three zones. The three-zone gradation pattern describes the probability peak of body radius—the radius of the largest body in each zone—rather than the radius distribution of all bodies.

2.1 Low-Velocity Zone (Outer Edge of the Solar System to Jupiter's Orbit) (Fig. 1)

(1) Spatial range. From the outer edge of the Solar System (Oort Cloud, about $5000AU to\ 10^5 AU$) inward to Jupiter's orbit (about 5.2 AU). Solar radiation flux is weakest in this zone.

(2) Dynamical characteristics. Orbital velocities are generally low, increasing from Neptune's 5.43 km/s to Jupiter's 13.06 km/s.

(3) Radius and morphological gradation. Physical radius R increases continuously as heliocentric distance r decreases. The sequence is interstellar molecules/small comets (diffuse state) → Kuiper Belt (semi-aggregated state, e.g., Eris, $R \approx 2400\ km$) → Neptune ($R = 24{,}750\ km$) → Uranus ($R = 25{,}900\ km$) → Saturn ($R = 60{,}000\ km$) → Jupiter (regional maximum, $R = 71{,}400\ km$) [2].

(4) Thermodynamic state. From outside inward, planets progressively develop significant intrinsic heat production; Jupiter and Saturn, for example, radiate more energy than they receive from the Sun [18].

2.2 Intermediate-Velocity Zone (Trojan Orbit to Earth's Orbit) (Fig. 1)

(1) Spatial range. From the Trojan asteroid orbit (5.2 AU) inward to Earth's orbit (1 AU). Solar radiation flux is intermediate.

(2) Dynamical characteristics. Orbital velocities increase markedly, from the Trojan asteroids' 13.06 km/s to Earth's 29.79 km/s [2].

(3) Radius and morphological gradation. Radius R continues to increase as r decreases: Trojan asteroids (diffuse state) → asteroid belt (e.g., Ceres, $R \approx 950\ km$) → Mars ($R = 3395\ km$) → Earth ($R = 6378\ km$, regional maximum) [2]. Jupiter is the evolutionary endpoint of the low-velocity zone, whereas the Trojan asteroids are the evolutionary starting point of the intermediate-velocity zone. They share an orbit and exhibit a mixed relationship. The increasing trend of radius and orbital velocity in the intermediate-velocity zone therefore cannot be counted from Jupiter; it must be counted from the Trojan asteroids.

(4) Density gradation. Mean density \rhoρ increases monotonically from Jupiter's 1.33 g/cm³ to Earth's 5.52 g/cm³ [2].

(5) Structural evolution. Inward, planetary interiors develop layered differentiation such as an asthenosphere, and geological activity increases.

2.3 High-Velocity Zone (Earth's Orbit to Mercury's Orbit) (Fig. 1)

(1) Spatial range. From Earth's orbit (1 AU) inward to Mercury's orbit (about 0.3 AU). Solar radiation flux is strongest in this zone.

(2) Dynamical characteristics. Orbital velocities are the highest in the Solar System, increasing from Earth's 29.79 km/s to Mercury's 47.89 km/s [2].

(3) Radius gradation. In contrast to the low- and intermediate-velocity zones, radius R decreases as r decreases: Earth ($R = 6378\ km$) → Venus ($R = 6050\ km$) → Mercury ($R = 2440\ km$) [2].

(4) Density characteristics. Mean density remains high (5.46–5.52 g/cm³) with no clear gradient.

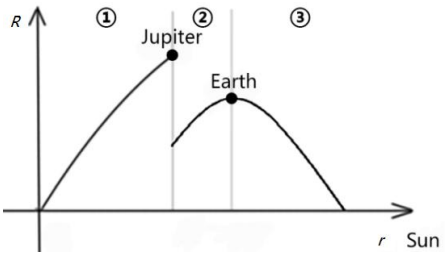


Fig. 1 Variation trend of celestial body radius in the Low-（①）, Medium-（②）, and High-Velocity（③）Zones.

Horizontal axis: direction approaching the Sun along the radial direction (heliocentric distance r decreasing); vertical axis: body radius R. In the low- and intermediate-velocity zones, R increases as r decreases; in the high-velocity zone, R decreases as r decreases.

2.4 Fundamental Difference Between the Three-Zone and Two-Zone Divisions

The traditional classification of Solar System planets uses a two-zone division: with the main asteroid belt as the boundary, planets are divided into inner planets (Mercury, Venus, Earth, Mars) and outer planets (Jupiter, Saturn, Uranus, Neptune). The three-zone division differs in that it analyzes all bodies in the Solar System—including diffuse states and asteroid belts—together with planets. It reveals a global gradation pattern that the two-zone division masks, making common regularities across regions more apparent and requiring a more general dynamical theory. The comparison shows the following.

(1) Body radius R varies non-monotonically with heliocentric distance r. The low- and intermediate-velocity zones share two features: first, in both zones, R increases as r decreases; second, morphological development proceeds from diffuse state → asteroid belt (semi-aggregated state) → smaller individual planet → larger individual planet. The evolutionary sequences of the two zones are similar in form but differ in starting point: the low-velocity zone starts from the diffuse state at the outer edge of the Solar System, while the intermediate-velocity zone starts from the Trojan asteroids co-orbiting with Jupiter.

(2) In contrast to the low- and intermediate-velocity zones, in the high-velocity zone R decreases as r decreases.

(3) The two turning points are Jupiter (about 5.2 AU) and Earth (about 1 AU).

2.5 Research Approach Derived from the Three-Zone Division

The three-zone division leads directly to the central question of this paper: does a new unified dynamical mechanism lie behind the three-zone gradation pattern?

First, in the low- and intermediate-velocity zones R increases as r decreases, whereas in the high-velocity zone R decreases as r decreases. Can this non-monotonic "increase then decrease" sequence be explained by a single dynamical component?

Second, globality. The theory applies not only to planets but also to all Solar System bodies, including diffuse states, asteroid belts, comets, and planetary rings. Traditional theory (gravity plus temperature gradient) can explain compositional differences among planets, but it cannot explain this cross-scale global gradation.

Third, the unified origin of the two extrema at Jupiter and Earth.

To address these questions, we introduce inlet–outlet structure theory, the element–environment relation, and the thrust formula, and use them to derive the three-zone gradation pattern.

3 Basic Theory of Exchange Mechanics

3.1 Matter Inlet–Outlet Structure Theory

In exchange mechanics, both macroscopic celestial bodies (such as Earth and the Moon) and microscopic particles (such as photons and electrons) evolve two basic functional units—inlets and outlets—to maintain matter and energy exchange with the external environment [9].

We define the structure responsible for absorbing matter and energy from the external environment as the inlet (denoted "−"). The absorbed matter–energy flow is the absorption flow (denoted J_{in}), and the equivalent mechanical action produced by absorption is the absorption force (denoted F_{in}), with the two related as $J_{\text{in}} \leftrightarrow F_{\text{in}}$. Correspondingly, the structure responsible for releasing matter and energy to the external environment is the outlet (denoted "+"). The released matter–energy flow is the release flow (denoted J_{out}), and the equivalent mechanical action produced is the release force (denoted F_{out}), denoted $J_{\text{out}} \leftrightarrow F_{\text{out}}$.

After matter and energy are absorbed through the inlet, they are transported some distance within the system and finally released outward through the outlet. Absorption flow and release flow are

collectively called exchange flow (J); absorption force and release force are collectively called exchange force (F_J).

Unified note. The content exchanged between inlet and outlet is collectively called exchange flow (J), including both matter flow and energy flow. Our focus is the electromagnetic radiation component of the energy flow: the dayside hemisphere absorbs solar electromagnetic radiation, and the nightside hemisphere releases the body's own electromagnetic radiation. The contribution of matter flow (such as solar wind and the interstellar medium) is not discussed in detail here and is left for future work.

If absorption and release coexist in a spatial region but absorption dominates ($J_{\text{in}} > J_{\text{out}}$), the region is an inlet region or absorption source. If release dominates ($J_{\text{out}} > J_{\text{in}}$), it is an outlet region or release source. This is the basic characteristic of the inlet–outlet structure: net flux dominance.

The quantitative difference between absorption flow and release flow is the flow difference (ΔJ). Taking the release direction as positive:

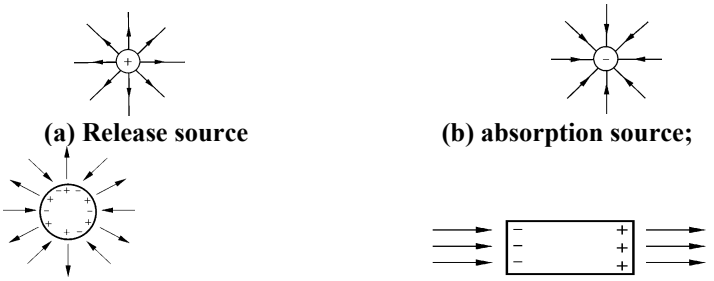
$$\Delta J = J_{\text{out}} - J_{\text{in}} \tag{3.1}$$

The difference between the corresponding absorption and release forces is the flow force difference (ΔF). Taking the release direction as positive:

$$\Delta F = F_{\text{out}} - F_{\text{in}} \tag{3.2}$$

3.2 Exchange Mechanics Transformation

In classical mechanics and relativity, Galilean and Lorentz transformations provide kinematic foundations by treating the object of study as a point mass. Exchange mechanics adopts a different systematic treatment: exchange mechanics transformation. This method classifies and partitions the object of study through the division into absorption source and release source and through identification of the inlet–outlet structure.



(a) Release source **(b) absorption source;**

(c) mixed inlet–outlet structure **(d) bipolar inlet–outlet structure**

Fig. 2 Four basic structures of exchange mechanics transformation. (a) Release source; (b) absorption source; (c) mixed inlet–outlet structure; (d) bipolar inlet–outlet structure.

Exchange mechanics transformation defines four basic conditions according to the structural characteristics of the system: (1) release source, a system dominated by release as a whole ($J_{\text{out}} > J_{\text{in}}$); (2) absorption source, a system dominated by absorption as a whole ($J_{\text{out}} < J_{\text{in}}$); (3) mixed inlet–outlet structure, in which inlet and outlet regions are spatially interwoven; and (4) bipolar inlet–outlet structure, in which inlet and outlet regions are concentrated at two geometrically opposite ends of the system (Fig. 2a–d).

This paper discusses only the effect of non-zero net thrust produced by the bipolar structure (day–night asymmetry).

4 Basic Assumptions of the Element–Environment Relation

Terminology. "Element–environment relation" denotes the theoretical relation $J \propto \rho$. "Element macroscopic distribution law" denotes the observational regularity that supports it, namely the interstellar molecular element distribution. The two stand in a theory–evidence relationship.

4.1 Observational Basis: Interstellar Molecular Element Distribution

Interstellar molecules occur mainly in macroscopic regions with extremely low matter–energy density (ρ) and very large spatial scales, such as ionized hydrogen regions, neutral hydrogen regions, dark nebulae, and supernova remnants [12]. Using interstellar molecular data confirmed by the late 1970s, frequency statistics of elemental composition—counting each element in a molecule only once—yield the following distribution regularities (Table 1) [7]:

Table 1 Examples of interstellar molecular composition (data source: [13])

CH	CH_3OH	H_2CS	SiS	CH_3CH_2CN	C_2H_4	CH_3C_2H	CH_3CH_2OH	HCN
CN	HCOOH	HNC	H_2CCHCN	HC_7N	CH_3COOH	HC_3N	C_2	H_2C_2O
CH^+	HCO^+	H_2S	$HCOOCH_3$	HC_9N	SO_2	CH_3SH	C_2H_2	CH_4
OH	$HCONH_2$	H_2CNH	NS	C_3H	SH_3CHO	HNO	CH_3NH_2	HCO
NH_3	CS	SO	NH_2CN	C_4H	H_2	$(CH_3)_2O$	CH_3CN	C_2H

H_2O	SiO	N_2H^+	HC_5N	NO	HNCS	HNCO	CO	OCS
HCHO								

(1) Periodic constraint. The elements involved are strictly limited to periods 1–3; period 4 and heavier elements have not been detected.

(2) Abundance trend. Occurrence frequencies are H(44) > C(42) > O(22) > N(21) > S(10) > Si(2).

(3) Position preference within periods. Except for hydrogen, the elements participating in molecular composition lie in the middle-to-late part of their periods (C, N, O, Si, S).

(4) Adjacency effect. Adjacent elements (such as H and C) have similar occurrence frequencies, whereas non-adjacent elements differ markedly.

The element abundance distribution in interstellar molecules (a low-\rhoρ environment), with clear periodicity and adjacency selectivity, strongly suggests that a physical quantity related to the intrinsic properties of elements governs their adaptive distribution in different ρ environments.

Note on data timeliness. The interstellar molecular data in Table 1 are as of the late 1970s [13]. In the decades since, the number of known interstellar molecules has increased from several dozen to more than 200 [14]. These newly discovered molecules include some containing period 4 and heavier elements, such as Fe- and Mg-bearing molecules, but the overall conclusion is unchanged.

4.2 Positive Correlation Between Exchange Quantity and Environmental Density

In exchange mechanics, the exchange quantity (J) of an element is its intrinsic intensity for maintaining steady-state existence through matter and energy exchange with the environment [7]. J is an intrinsic property of the element, characterizing the baseline intrinsic exchange intensity required for its atomic nucleus to maintain structural stability under an ideal equilibrium fully matched to the environment [7]. We adopt the following working hypothesis: the exchange quantity (J) of an element is positively correlated with the comprehensive density (ρ) of matter (M) and energy (E) in the environment most suitable for its existence:

$$J \propto \rho(M \cup E) \tag{4.1}$$

Basis and limitations. The most direct observational basis comes from the element distribution of interstellar molecules: in interstellar environments with extremely low matter and energy density, the elements involved in detected molecules are mainly from periods 1–3 [7]. This fact admits at least two alternative explanations: (a) heavy elements have very low abundance in the interstellar medium, since cosmic abundance decreases with atomic number; and (b) heavy elements are difficult to form detectable molecular spectral lines. We have not ruled out these alternatives, and we therefore treat Eq. (4.1) as a working hypothesis rather than an axiom.

Falsification path. If in some celestial body system the element distribution systematically contradicts the trend predicted by $J \propto \rho$ —for example, if high-J elements dominate in a low-ρ environment and no other mechanism can explain it—then the hypothesis requires revision or abandonment.

Environmental density ρ can be divided into three basic types according to its spatiotemporal variation:

(1) Decreasing environment ($\boldsymbol{\rho \to -}$). Matter and energy density decrease continuously along a fixed direction, as in the Solar System along the radial direction away from the Sun.

(2) Increasing environment ($\boldsymbol{\rho \to +}$). Density increases continuously along a fixed direction, as in the Solar System along the direction approaching the Sun.

(3) Steady environment ($\boldsymbol{\rho \to \pm}$). Density remains relatively constant in space and time.

For the Solar System we define a direction: approaching the Sun is inward, and the opposite is outward.

4.3 Periodic Gradation of Exchange Quantity and Environmental Adaptability

From the definition of J and the classification of ρ, the adaptive distribution of elements in different environments follows [7,8]:

(1) Cross-period trend. Low-period elements (periods 1–3) have smaller J values and are better adapted to low-ρ environments such as interstellar space. High-period elements (period 4 and above) have larger J values and are better adapted to high-ρ environments such as those near stars. In a decreasing environment ($\rho \to -$), the probability PP of element adaptability decreases with increasing period number.

(2) Same-period trend. Within a period, the exchange quantity J decreases with increasing atomic number Z. Therefore, in a decreasing environment ($\rho \to -$), the existence probability P of elements within a period increases with increasing Z.

(3) Adjacency principle. Adjacent elements in the periodic table have similar J values and therefore similar environmental adaptability [7].

Note on dimensions. Quantifying J—its dimension, measurement method, and relation to known physical quantities—is an important direction for future work. At the element level, J may refer to atomic weight, that is, the dimension of mass, with the difference that within a period the numerical value of J varies monotonically in the direction opposite to increasing atomic number, while across the periodic table it increases from low to high periods. At the planetary level, the dimension of mass ([kg]) can be adopted directly. In $J \propto \rho$ (Eq. 4.1), J has dimension [kg] and ρ has dimension [kg/m³]; the dimensions are inconsistent. Here "$\propto$" denotes a trend scaling relation, not a dimensionally strict equality. Scaling relations between quantities of different dimensions are common in science.

4.4 Direct Corollaries for the Composition of Solar System Bodies

This chapter establishes the element–environment relation ($J \propto \rho$, Eq. 4.1): the exchange quantity of an element is positively correlated with the density of the environment most suitable for its existence. This relation provides the material basis for the thrust formula in Chapter 5.

In the Solar System, the environmental matter–energy density ρ has a clear radial gradient: ρ increases as heliocentric distance decreases. From Eq. (4.1) and the three laws in Section 4.3, two basic rules for body composition follow directly.

(1) Inner-region bodies should be dominated by high-J heavy elements. Mercury, Venus, Earth, and Mars should consist mainly of high-J elements such as iron, silicon, magnesium, and oxygen, and should therefore have high mean density. This prediction agrees with observations.

(2) Outer-region bodies should be dominated by low-J light elements. Jupiter, Saturn, Uranus, and Neptune should consist mainly of low-J elements such as hydrogen and helium, and should therefore have low mean density. This prediction also agrees with observations.

The density differences of Solar System bodies depend mainly on the temperature gradient at formation—condensation lines of volatile substances—and on subsequent gravitational accretion [15,6]. Eq. (4.1) does not contradict this standard picture; it provides a complementary perspective on the adaptive distribution of elements.

5 Net Thrust Formula: Geometric Difference Between Sphere and Hemisphere

5.1 Physical Basis: Electromagnetic Waves Carry Momentum

As noted in Section 3.1, the content exchanged through the inlet–outlet structure includes matter flow and energy flow. The thrust formula developed here focuses on the electromagnetic radiation component of the energy flow: the dayside hemisphere absorbs solar electromagnetic radiation, and the nightside hemisphere releases the body's own electromagnetic radiation. We now derive the net thrust formula from the first principle that electromagnetic waves carry momentum.

Electromagnetic waves (photons) carry momentum. For an isotropic Lambertian surface, the net momentum radiated per unit area per unit time is directed along the outward normal and has magnitude

$$\frac{dF}{dA} = \frac{2}{3} \cdot \frac{\varepsilon\sigma T^4}{c} \cdot \hat{n} \qquad (5.1)$$

Derivation. Let the radiation intensity be I $(W \cdot m^{-2} \cdot sr^{-1})$. The power radiated within solid angle $d\Omega$ in a direction making an angle θ' with the normal is $dP = I \cos\theta' d\Omega dA$. The corresponding momentum is dP/c, directed along the radiation direction. Integrating over the entire hemispherical space gives $dF/dA = (2\pi I/3c)n^{\wedge}$. From the Stefan–Boltzmann law $M = \pi I = \varepsilon\sigma T^4$, substitution yields Eq. (5.1).

Key point. Eq. (5.1) is identical for solar radiation, planetary radiation, and atomic radiation, because all are electromagnetic waves and all obey the same momentum–energy relation. This microscopic homology is discussed in Section 5.7.

5.2 Complete Sphere: Net Force Strictly Zero

Let the sphere radius be R and the surface temperature be constant at T. The normal at any point on the sphere is

$$\hat{n}(\theta, \varphi) = (\sin\theta\cos\varphi, \sin\theta\sin\varphi, \cos\theta) \qquad (5.2)$$

The net radiation force of the sphere is

$$F_{\text{sphere}} = \oint_{\text{sphere}} \frac{2}{3} \cdot \frac{\varepsilon\sigma T^4}{c} \cdot \hat{n}\, dA \qquad (5.3)$$

Because T is constant, $n^{\wedge}$ appears in opposite pairs on the sphere, and the integral is strictly zero:

$$F_{\text{sphere}} = 0 \qquad (5.4)$$

Physical meaning. The Sun, as a complete sphere, has zero net recoil force from its own radiation. A planet, as a complete sphere, also has zero net recoil force from its total own radiation. In this respect the Sun and planets are completely symmetric.

The strict zero in Eq. (5.4) depends on the assumption that surface temperature T is constant. For real bodies, surface temperature is spatially inhomogeneous—sunspots and planetary day–night temperature differences, for example—and the spherical integral is not necessarily zero; it depends on the specific form of the temperature distribution. Our focus is the macroscopic temperature difference at

the hemispheric scale, that is, the difference between dayside and nightside hemispheres, rather than microscopic surface temperature fluctuations. Under macroscopic averaging at the hemispheric scale, Eq. (5.4) holds approximately.

5.3 Hemispherical Surface: Net Force Strictly Non-Zero

Consider the nightside hemisphere. Let the solar direction be $+z$, so the nightside hemisphere is the surface $z < 0$, with polar angle $\theta \in [\pi/2, \pi]$.

The net radiation force of the nightside hemisphere is

$$F_{\text{night}} = \int_{\text{night}} \frac{2}{3} \cdot \frac{\varepsilon\sigma T^4}{c} \cdot \hat{n}\, dA \qquad (5.5)$$

The x and y components vanish after integration over azimuth φ, so only the zz component is needed. The z component of the normal is $\cos\theta$, and the area element is $dA = R^2 \sin\theta\ d\theta d\varphi$:

$$F_{\text{night},z} = \frac{2}{3} \cdot \frac{\varepsilon\sigma T^4}{c} \cdot 2\pi R^2 \int_{\pi/2}^{\pi} \cos\theta \sin\theta\ d\theta \qquad (5.6)$$

Evaluating the integral:

$$\int_{\pi/2}^{\pi} \cos\theta \sin\theta\ d\theta = \frac{\sin^2\theta}{2} = \frac{0-1}{2} = -\frac{1}{2} \qquad (5.7)$$

Therefore,

$$F_{\text{night},z} = -\frac{2\pi R^2}{3} \cdot \frac{\varepsilon\sigma T^4}{c} < 0 \qquad (5.8)$$

The negative sign indicates the direction along $-z$, that is, toward the Sun.

5.4 Key Point: Why the Sphere Is Zero and the Hemisphere Is Not

This is the mathematical basis of the paper's core contribution, and it should be stated explicitly.

Sphere. The normal $n^\wedge$ covers the entire 4π solid angle. For every normal $n^\wedge$, the opposite direction $-n^\wedge$ corresponds to the normal at another point on the sphere. The integrand $n^\wedge$ therefore appears in opposite pairs, and the integral cancels strictly to zero.

Hemisphere. The normal covers only 2π solid angle, the half-space $z < 0$. The opposite direction of every nightside normal falls on the dayside hemisphere, not on the nightside hemisphere. The integrand $n^\wedge$ therefore does not appear in opposite pairs on the nightside hemisphere, the integral does not cancel, and the result is non-zero, directed toward the Sun.

Geometric configuration	Normal coverage	Opposite pairs?	Net force
Complete sphere	Entire 4π	Yes	Strictly zero
Hemispherical surface	Half 2π	No	Non-zero (direction set by geometry)

The integral results for a sphere and a hemisphere are therefore completely different: the sphere is zero, and the hemisphere is non-zero. This is a purely geometric result and does not rely on additional assumptions.

5.5 Dayside Hemisphere, Reflection Term, and Net Thrust Formula

(1) Force of the dayside hemisphere

The net radiation force of the dayside hemisphere ($\theta \in [0, \pi/2]$) is

$$F_{\text{day,rad}} = +\frac{2\pi R^2}{3} \cdot \frac{\varepsilon_{\text{day}}\sigma T_{\text{day}}^4}{c} > 0 \qquad (5.9)$$

The positive sign indicates the direction along $+z$, away from the Sun.

(2) Contribution of the reflection term

In addition to its own thermal radiation, the dayside hemisphere reflects part of the sunlight. The momentum transfer of reflected light is

$$F_{\text{day,refl}} = \frac{\pi R^2 F_\odot A}{c} \cdot \kappa \qquad (5.10)$$

where A is albedo, $F_\odot$ is the solar constant, and κ is the reflection direction factor:

Specular reflection: $\kappa = 2$ (light reverses; momentum change $2p$);

Diffuse reflection (Lambertian): $\kappa = 2/3$ (after hemispheric integration, net momentum along the normal).

For specular reflection the direction is toward the Sun; for diffuse reflection it is away from the Sun.

Eq. (5.10) represents two simplified limiting cases. Real planetary surface reflection is neither completely specular nor completely Lambertian, but intermediate. A more rigorous description requires

the bidirectional reflectance distribution function (BRDF), which is beyond the scope of this paper. For low-albedo bodies the reflection term can be neglected; for high-albedo bodies such as Venus ($A \approx 0.7$) it cannot.

(3) Net thrust formula

The total net radiation force of a planet is therefore

$$F_{\text{net}} = F_{\text{day,rad}} + F_{\text{day,refl}} - |F_{\text{night}}| \tag{5.11}$$

Expanding,

$$F_{\text{net}} = \frac{2\pi R^2}{3c}\left(\varepsilon_{\text{day}}\sigma T_{\text{day}}^4 - \varepsilon_{\text{night}}\sigma T_{\text{night}}^4\right) + \frac{\pi R^2 F_{\odot} A}{c}\kappa \tag{5.12}$$

Direction criterion.

If $T_{\text{day}} > T_{\text{night}}$(dayside hotter), the first term is positive and the net thrust points away from the Sun.

If $T_{\text{night}} > T_{\text{day}}$(nightside hotter, as for giant planets and planetesimals), the first term is negative and the net thrust points toward the Sun.

The reflection term points away from the Sun for diffuse reflection and toward the Sun for specular reflection; its magnitude is far smaller than the first term for low-albedo bodies.

Simplified form. For low-albedo bodies with significant day–night temperature differences, the reflection term can be neglected and the net thrust formula simplifies to

$$F_{\text{net}} \approx \frac{2\pi R^2}{3c}\left(\varepsilon_{\text{day}}\sigma T_{\text{day}}^4 - \varepsilon_{\text{night}}\sigma T_{\text{night}}^4\right) \tag{5.13}$$

For high-albedo bodies such as Venus ($A \approx 0.7$), the reflection term cannot be neglected and the complete formula (5.12) must be used.

5.6 Energy Balance and Temperature Constraints

T_{day} and T_{night} in Eq. (5.12) are not independent variables; they are set by the energy budget of the body. The energy balance equations for the dayside and nightside hemispheres are as follows.

(1) Dayside hemisphere energy balance

The power absorbed by the dayside hemisphere from solar radiation is $P_{\text{abs}} = \pi R^2 F_{\odot}(1 - A)$, and the thermal power radiated outward is $P_{\text{rad,day}} = 2\pi R^2 \varepsilon\sigma T_{\text{day}}^4$. The share of internal heat source P_{int} allocated to the dayside hemisphere is $P_{\text{int,day}}$, and the day–night heat transport term is $P_{\text{transport}}$. In steady state,

$$\pi R^2 F_{\odot}(1 - A) + P_{\text{int,day}} - P_{\text{transport}} = 2\pi R^2 \varepsilon\sigma T_{\text{day}}^4 \tag{5.14}$$

(2) Nightside hemisphere energy balance

The nightside hemisphere receives no solar radiation; its energy sources are the internal heat source $P_{\text{int,night}}$ and day–night heat transport $P_{\text{transport}}$:

$$P_{\text{int,night}} + P_{\text{transport}} = 2\pi R^2 \varepsilon\sigma T_{\text{night}}^4 \tag{5.15}$$

(3) Temperature solution

From Eqs. (5.14) and (5.15),

$$T_{\text{day}} = \left[\frac{F_{\odot}(1 - A) + 2P_{\text{int,day}}/(\pi R^2) - 2P_{\text{transport}}/(\pi R^2)}{2\varepsilon\sigma}\right]^{1/4} \tag{5.16}$$

$$T_{\text{night}} = \left[\frac{P_{\text{int,night}} + P_{\text{transport}}}{2\pi R^2 \varepsilon\sigma}\right]^{1/4} \tag{5.17}$$

(4) Influence of heat transport on different bodies

Airless bodies (Mercury, Moon): $P_{\text{transport}} \approx 0$, with extremely large day–night temperature differences.

Bodies with atmospheres (Earth, Venus): $P_{\text{transport}}$ is significant and the day–night temperature difference is reduced.

Giant planets (Jupiter, Saturn): $P_{\text{transport}}$ is dominated by convection and the day–night temperature difference is extremely small.

(5) Two cases of internal heat distribution

No significant internal heat (Moon, asteroids): $P_{\text{int}} \approx 0$, $T_{\text{night}} \approx 0K$, and T_{day} is set by solar radiation. Here $F_{\text{net}} > 0$: dayside thermal radiation dominates and points away from the Sun.

Significant internal heat (Jupiter, Saturn, early planetesimals): P_{int} is significant, $T_{\text{night}} > 0K$, and possibly $T_{\text{night}} > T_{\text{day}}$. Here $F_{\text{net}} < 0$: nightside thermal radiation dominates and points toward the Sun.

(6) Critical internal heat power and stable orbit

The condition $F_{\text{net}} = 0$ is

$$\varepsilon_{\text{day}}\sigma T_{\text{day}}^4 = \varepsilon_{\text{night}}\sigma T_{\text{night}}^4 \tag{5.18}$$

Substituting Eqs. (5.16) and (5.17) gives the critical internal heat power:

$$P_{\text{int,crit}} \approx \frac{\pi R^2 F_{\odot}(1 - A)}{2} \tag{5.19}$$

When solar radiation interacts with planetary nightside radiation, three cases arise:

$F_{\text{net}} < 0$ (toward the Sun): nightside radiation force dominates and the planet tends to move inward;

$F_{\text{net}} > 0$ (away from the Sun): dayside radiation force dominates and the planet tends to move outward;

$F_{\text{net}} = 0$: the two forces balance and the planet is in a stable orbit.

The present planets are in the state $F_{\text{net}} = 0$, maintaining stable orbits after modulation.

We now show that the electromagnetic radiation on which the thrust formula depends has a common microscopic origin at the solar, planetary, and atomic scales.

5.7 Microscopic Homology of Electromagnetic Radiation

Eqs. (5.1)–(5.13) apply equally to solar radiation, planetary radiation, and atomic radiation, because all are electromagnetic waves and all carry momentum. The differences among them lie only in macroscopic parameters:

Object	Temperature	Peak wavelength	Radiation power	Geometric configuration
Sun	~5800 K	~500 nm (visible)	$3.8 \times 10^{26} W$	Complete sphere (zero net force)
Planet	100–700 K	4–30 μm (infrared)	$10^{13} - 10^{17} W$	Sphere (total net force from Eq. 5.12)
Atom	Quantum transition	Discrete lines	Extremely small	Isotropic (zero net force)

The microscopic mechanism is fully homologous. All electromagnetic radiation comes from the accelerated motion of charged particles: electron transitions in atoms, molecular rotation and vibration, bremsstrahlung of free electrons in plasma, and lattice thermal vibration in solids. The differences are as follows:

A single atom radiates discrete spectral lines, isotropically, with zero net force.

A large collection of atoms (a planetary surface) produces a continuous spectrum (blackbody spectrum), and the geometric configuration determines the net force.

A stellar interior is a high-temperature dense plasma; its radiation is a continuous spectrum, spherically symmetric, with zero net force.

"Atomic radiation" and "planetary radiation" are therefore not two mechanisms but manifestations of the same mechanism at different scales, densities, and temperatures. Planetary blackbody radiation is essentially the superposition of collective radiation from a large number of atoms inside the body. The inlet–outlet hypothesis of this paper rests on this unified microscopic basis.

5.8 Applicability and Order of Magnitude of the Thrust Formula

Eq. (5.13) applies to all macroscopic or microscopic bodies in different regions of the Solar System, including planets, dwarf planets, asteroids, comets, and dust particles.

Order-of-magnitude estimate (Earth). $R = 6.378 \times 10^6 m$, $T_{\text{day}} \approx 288K$, $T_{\text{night}} \approx 280K$, $\varepsilon \approx 1$:

$$F_{\text{net}} \approx \frac{2\pi(6.378 \times 10^6)^2}{3 \times 3 \times 10^8} \times 5.67 \times 10^{-8} \times (288^4 - 280^4) \approx 10^7\ N$$

The solar gravitational force on Earth is about $3.5 \times 10^{22} N$, so $F_{\text{net}}/F_{\text{grav}} \approx 10^{-15}$.

Order-of-magnitude estimate (early planetesimals). $R \approx 10 - 1000km$, $P_{\text{int}} \approx 10^{14} - 10^{16} W$ from ^{26}Al decay and accretion residual heat [16], and $F_{\text{net}}/F_{\text{grav}}$can reach $10^{-2} - 10^{0}$, so thrust and gravity can be of the same order.

Explicit limitation of the applicable stage.

(1) Early planetesimal aggregation stage (about $10^6 - 10^7$ years after Solar System formation). Thrust and gravity are of the same order ($F_{\text{net}}/F_{\text{grav}} \approx 10^{-2} - 10^{0}$) and may have substantially influenced the radial distribution of planetesimals. This is the main applicable stage for the derivations in Chapters 6 and 7.

(2) Current planetary stage. $F_{\text{net}}/F_{\text{grav}} \approx 10^{-15}$, and thrust is only a minor modulation, insufficient to explain directly the present macroscopic configuration of the planets. The discussions in Chapters 6 and 7 of the current planetary radius–density–rotation sequence should be read as possible imprints left by thrust effects during the early stage, not as evidence that present thrust directly determines planetary configuration.

(3) Current small bodies with significant internal heat (such as active comets). Thrust may produce observable tiny perturbations in their orbits, but the magnitude still requires specific estimation.

The thrust formula itself applies to bodies of all scales, which is the basis for the universality of the three-zone gradation pattern. Its quantitative explanatory power, however, is limited to the early planetesimal stage. This limitation does not affect the core contributions of the paper: the geometric derivation of the thrust formula (Sections 5.2–5.4) is rigorous; the empirical pattern of three-zone gradation (Chapter 2) summarizes observational facts; and the falsification paths (Chapter 9) are explicit.

5.9 Physical Expression of the Thrust Formula and Its Compatibility with the Gravitational Formula

We now express the physical meaning of the net thrust in a more convenient form.

For a planet, the "absorption" it experiences comes essentially from solar radiation—the energy radiated outward by the Sun pushes the planet. The planet's own "release" comes from the outward radiation of heat from its interior. To adapt to the environmental density $\rho(r)$ at different heliocentric distances, the planet mainly adjusts its own release power to balance the equivalent action caused by solar radiation. The same applies to other bodies.

The net thrust of a planet is defined as the difference between the momentum flux of its own released radiation and the equivalent action caused by solar radiation:

$$F_{\text{net}} = \left|F_p^+ - F_\odot^+\right| \qquad (5.20)$$

By Newton's second law, the radial acceleration a_r of the planet relative to the Sun satisfies

$$a_r = \frac{F_{\text{net}}}{m} \qquad (5.21)$$

The physical positioning of the thrust formula should be clear. As stated in Chapter 1, gravity dominates the kinematics of planetary revolution, while thrust modulates the radial equilibrium position of the planet in the Solar System. The thrust in Eq. (5.20) is not the driving force of planetary revolution; it is the modulating force that determines the heliocentric distance at which the planet reaches radial equilibrium.

Observations show that for the eight planets from Mercury to Neptune, orbital velocity decreases monotonically with increasing heliocentric distance (Table 2) and has no clear correlation with planetary mass [2]. This is a kinematic law already explained by Newtonian mechanics: by Kepler's third law, given the orbital radius, the orbital velocity is determined. What the net thrust theory aims to explain is a different question: why are the planets distributed at their present heliocentric distances? The orbital position of a planet is mainly determined by its net thrust F_{net}. A planet with a larger net thrust can overcome stronger solar radiation action and enter a closer, faster orbit; otherwise it remains in a distant, low-speed orbit.

Notably, the conclusion that a planet with a larger net thrust enters a closer, faster orbit is kinematically compatible with Kepler's third law under the gravitational path ($v \propto r^{-1/2}$). In describing the relation between planetary orbital velocity and heliocentric distance, the thrust formula and the gravitational formula are therefore compatible. Their physical mechanisms differ—gravity describes centripetal binding, whereas thrust describes radial modulation—but they give compatible results at the kinematic level. This compatibility indicates that the thrust formula is not a replacement for the gravitational formula but another descriptive perspective on the same physical reality.

6 Derivation of Celestial Body Gradation Motion

6.1 Low-Velocity Zone

6.1.1 Scaling Relation Between Thrust and Celestial Body Radius

As noted in Section 5.8, the derivation in this chapter applies to the early planetesimal aggregation stage. In the low-velocity zone, solar radiation flux is relatively weak. The dynamical process of a celestial body can be compared to a train running at low speed: its motion is less affected by external "air resistance" (solar radiation action), and increasing the number of exchange units is an effective way to increase the total release force linearly. The dayside hemisphere of a celestial body mainly absorbs solar radiation and can be regarded as an inlet; the nightside hemisphere mainly releases its own radiation and can be regarded as an outlet. Under these conditions the entire celestial body can be regarded as having a bipolar inlet–outlet structure (Fig. 3).

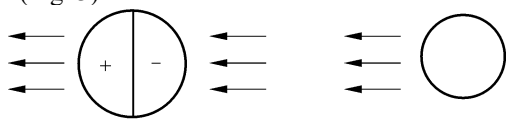


Fig. 3 Absorption source with a bipolar inlet–outlet structure (left) and release source (right).

Let a celestial body BB with a bipolar inlet–outlet structure consist of nn exchange units, and let the release force of each unit cc be $p_{c,\text{out}}$. Neglecting coupling resistance between units, the total release force of the celestial body is approximately the linear superposition of the release forces of the units:

$$P_{B,\text{out}} \approx \sum_i p_{c,i,\text{out}} \qquad (6.1)$$

When the exchange units are continuously distributed along a radial path ll, they can be treated as a one-dimensional superposition model:

$$P_{B,\text{out}} = \int_0^R p_{\text{out}}(l')\, dl' \qquad (6.2)$$

If $p_{\text{out}}(l)$ is approximately uniform within the celestial body, this simplifies to

$$P_{B,\text{out}} \propto R \qquad (6.3)$$

Eq. (6.3) indicates that in the low-velocity zone, the total release force of a celestial body is proportional to its radius. This scaling relation describes the evolutionary path from diffuse interstellar matter in the Oort Cloud, to the Kuiper Belt, and finally to giant planets such as Jupiter and Saturn.

On the relation between radial distribution and the bipolar surface structure. Eqs. (6.1)–(6.3) treat a celestial body as a radially layered exchange medium, with each layer contributing $p_{\text{out}}(l)dl$, so that the total release force is $\propto R$. This is complementary to the surface geometry of the bipolar inlet–outlet structure (dayside inlet, nightside outlet):

Radial layering describes energy transport and release inside the celestial body.

The bipolar surface structure describes the inlet–outlet distribution on the celestial body's surface (dayside absorption, nightside release).

The energy of radial layering is ultimately released to the external environment through the bipolar surface structure.

The two pictures are therefore not contradictory; they describe the same physical process at different levels.

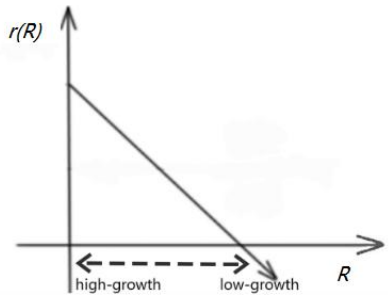


Fig. 4 Schematic diagram of the variation of the growth rate of the releasing force, γ(R), as a function of the planetary body's radius, *R*.

(The vertical axis: γ(R); the horizontal axis: R; the curve illustrates the decreasing trend of γ(R) with R increases.)

6.1.2 Constraint Relation Between Release Force Growth Rate and Radius

(1) Loss of release force to internal resistance

In a real celestial body, internal energy transport encounters resistance. This resistance R_{int} increases with transport path l:

$$R_{\text{int}}(l) = \int_0^l \xi(s)\, ds \qquad (6.4)$$

where $\xi(s)$ is the resistance coefficient per unit length. If ξ is constant, then $R_{\text{int}} \propto l$. The net release force after accounting for internal loss is therefore

$$P_{\text{net,out}} = P_{B,\text{out}} - R_{\text{int}}(l) \qquad (6.5)$$

As radius R increases, resistance R_{int} grows faster than the total release force, so the growth rate of the net release force decreases with increasing RR. When the radius reaches a critical value, the net release power saturates and no longer increases with scale. Jupiter (71,492 km) is the manifestation of this critical scale in the low-velocity zone, forming the maximum of that zone.

(2) Interval characteristics of the radius change rate (Fig. 4)

Define the release force growth rate $\gamma(R) = dP_{\text{net,out}}/dR$. According to how $\gamma(R)$ varies with R, two characteristic intervals can be distinguished:

a. High-growth region. When R is relatively small, $\gamma(R)$ is relatively large, so a small increase in radius produces a significant increase in thrust.

b. Low-growth region. When R is relatively large, $\gamma(R)$ is relatively small, so a large increase in radius is required for a significant thrust increment.

For the eight planets as a whole, the zoning of $\gamma(R)$ is as follows:

Mercury: smallest radius ($R = 2440\ km$), relatively in the high-growth region;

Saturn and Jupiter: relatively large radii ($R = 60{,}000$ and $71{,}400$km), relatively in the low-growth region.

In the low-velocity zone, Uranus and Neptune have relatively small radii ($R = 25{,}900$ and $24{,}750$ km) and are relatively in the high-growth region; Saturn and Jupiter are relatively in the low-growth region.

Table 2 Basic parameters of the eight planets (data source: [2])

Planet	Avg. Distance to Sun (Million km)	Equatorial Radius (km)	Orbital Period	Rotation Period	Avg. Orbital Speed (km/s)	Mass (Earth=1)	Volume (Earth=1)	Avg. Density (g/cm³)	Moons	Rings
Mercury	57.9	2,440	87.9 d	58.6 d	47.89	0.05	0.056	5.46	0	-
Venus	108.2	6,050	224.7 d	243 d	35.03	0.82	0.856	5.26	0	-
Earth	149.6	6,378	1 y	23h 56m	29.79	1.00	1.000	5.52	1	-
Mars	227.9	3,395	1.9 y	24h 37m	24.13	0.11	0.150	3.96	2	-
Jupiter	778.0	71,400	11.8 y	9h 50m	13.06	317.94	1316	1.33	16	Yes
Saturn	1427.0	60,000	29.5 y	10h 14m	9.64	95.18	745	0.70	21-23	Yes
Uranus	2870.0	25,900	84.0 y	~16h	6.81	14.63	65.2	1.24	15	Yes
Neptune	4496.0	24,750	164.8 y	~18h	5.43	17.22	57.1	1.66	3	Yes

6.1.3 Constraints of Macroscopic Element Distribution on Density

Giant planets in the low-velocity zone generally show density-decreasing layered structures: a high-density core (ρ_{core}) surrounded by a low-density outer layer (ρ_{layer}). Assuming a constant density difference between core and outer layer for similar planets, $\rho_{\text{core}} - \rho_{\text{layer}} = \Delta\rho$, the mean density $\bar{\rho}(R)$ of a celestial body is the radial average of its internal density distribution $\rho(r)$:

$$\bar{\rho}(R) = \frac{3}{R^3}\int_0^R \rho\,(r) r^2\, dr \qquad (6.6)$$

Because $\rho(r)$ is a decreasing function, $\bar{\rho}(R)$ decreases with increasing radius R. The mean density of celestial bodies in the low-velocity zone therefore decreases systematically as heliocentric distance decreases and body radius increases (Table 2): Pluto \sim 1.85~1.85 g/cm³ → Neptune 1.66 → Uranus 1.24 → Saturn 0.70 g/cm³ [2].

This density gradation provides an observational test of the element distribution law. If distant large-radius bodies were assumed to have the same density as smaller bodies, their cores would necessarily consist of heavier elements, violating the basic constraint of the element macroscopic distribution law that heavy elements are difficult to enrich in low-\rhoρ environments [7]. Density decrease is therefore not accidental but an inevitable manifestation of the element distribution law at the celestial body scale.

6.2 Intermediate-Velocity Zone

6.2.1 Restart of the Gradation Pattern and Element Transition

In the low-velocity zone, celestial bodies increase their net release force by increasing radius, with light elements as the physical carrier. When the radius grows to the Jupiter scale, however, the sharp increase in internal resistance causes the release force growth rate $\gamma(R)$ to approach zero or even become negative, so the evolutionary path that relies solely on increasing scale becomes ineffective.

According to the element–environment relation (Eq. 4.1), environmental matter–energy density ρ increases as heliocentric distance decreases, and the stable existence probability of heavy elements with high exchange quantity J in the near-Sun (high-ρ) region increases significantly. Celestial body evolution in the intermediate-velocity zone therefore adopts a new strategy: replacing the physical carrier and rebuilding the body on a heavy-element basis.

Let the mean exchange quantities of light and heavy element matrices be J_L and J_H, respectively, with $J_H > J_L$. Under the equilibrium condition of achieving the same release force F_{out}, the higher exchange output efficiency per unit volume of heavy elements means that the effective force-bearing area S, and hence the radius R, required for a body composed of them is smaller:

$$S(J_H) < S(J_L) \Rightarrow R(J_H) < R(J_L) \qquad (6.7)$$

Within Jupiter's orbit, therefore, the celestial body evolutionary sequence can restart on the new physical basis of heavy elements: from the Trojan asteroids near Jupiter's orbit (diffuse state) → main asteroid belt (semi-aggregated state) → Mars → Earth (regional radius maximum).

6.2.2 Unified Origin of the Two Extrema

The maximum of the low-velocity zone (Jupiter, 71,400 km) and the maximum of the intermediate-velocity zone (Earth, 6,378 km) are manifestations of the same mechanism on two physical carriers.

(1) Common mechanism. From the diffuse state inward, body radius increases continuously, the energy transport path lengthens, and the resistance loss $R_{\text{int}}(l) \propto l$ increases, so the release force growth rate $\gamma(R)$ decreases. When the radius reaches a critical value, $\gamma(R)$ approaches zero and the radius can no longer increase.

(2) Origin of the scale difference. Jupiter is the dissipation limit of the light-element carrier, and Earth is the dissipation limit of the heavy-element carrier. From Eq. (6.7), the exchange output efficiency

per unit volume of heavy elements is higher, so the body radius required to achieve the same release force is smaller.

6.2.3 Systematic Comparison Between the Low- and Intermediate-Velocity Zones

Dimension	Low-velocity zone	Intermediate-velocity zone
Physical carrier	Light elements	Heavy elements
Evolutionary starting point	Diffuse state at the outer edge of the Solar System	Trojan asteroids (co-orbiting with Jupiter)
Evolutionary endpoint	Jupiter (71,400 km)	Earth (6,378 km)
Dissipation limit mechanism	Decreasing $\gamma(R)$	Decreasing $\gamma(R)$
Cause of scale difference	Low exchange output efficiency of light elements	High exchange output efficiency of heavy elements

6.3 High-Velocity Zone

6.3.1 Mantle Asthenosphere and Energy Constraint of the Radius Maximum

Earth is the radius maximum in the transition from the intermediate-velocity zone to the high-velocity zone. Its internal matter–energy exchange flow F_{out} produces significant viscous dissipation and heat accumulation during long-distance transport. When the release flow transport path l reaches a critical length l_{soft}, the volumetric heating rate q from internal dissipation ($q \propto R^3$) exceeds the melting threshold of upper mantle rocks, causing partial melting of mantle material and forming an asthenosphere on a global scale.

6.3.2 Dynamical Mechanism of Radius Decrease in the High-Velocity Zone

Two different mechanisms should be distinguished: the origin of the two extrema, which reflects the dissipation limit caused by decreasing $\gamma(R)$, and the origin of radius decrease in the high-velocity zone, which reflects thrust-to-weight ratio optimization caused by enhanced solar radiation action.

(1) Scale constraint under a strong radiation environment. In the high-velocity zone ($r < 1$ AU), solar radiation flux increases sharply as heliocentric distance r decreases (of order $\propto r^{-2}$). Solar radiation action becomes the dominant factor constraining body configuration.

(2) Double maxima and internal dissipation limit. The Solar System has two characteristic radius maxima: Jupiter, the dissipation limit of the light-element carrier, and Earth, the dissipation limit of the heavy-element carrier.

(3) Thrust-to-weight ratio optimization and negative correlation with radius. Define the relative thrust-to-weight ratio Γ of a celestial body as the ratio of its net thrust to mass:

$$\Gamma = \frac{F_{\text{net}}}{mg} \tag{6.8}$$

The value of Γ defined by Eq. (6.8) is extremely small at the celestial body scale; Earth's Γ, for example, is about 10^{-15}. "Thrust-to-weight ratio optimization" is therefore relative: under the strong radiation environment of the high-velocity zone, bodies with smaller radii have relatively higher thrust per unit mass. It is not an active behavior of celestial bodies but the result of natural selection.

In the high-velocity zone, celestial bodies composed mainly of heavier elements with approximately constant mean density $\bar{\rho}$ adopt the high-growth-region adaptation of the release force growth rate $\gamma(R)$, reducing their physical radius to increase the relative thrust-to-weight ratio Γ. This explains the reverse-order radius decrease of bodies in the high-velocity zone.

6.3.3 Extreme Effect of Mercury's Sharp Radius Decrease

In the high-velocity zone, Mercury is a typical case in which relative thrust-to-weight ratio optimization reaches an extreme. Earth lies in the low-growth region of $\gamma(R)$: its radius is large, but the thrust gain per unit scale increase is small. Mercury, through drastic radius reduction, jumps to the high-growth region of $\gamma(R)$.

The relative sharp decrease of Mercury's radius is dynamically the reverse of the significant radius increase from Saturn to Jupiter. Both are driven by the zoning characteristics of the release force growth rate $\gamma(R)$ as a function of radius R.

7 Environmental Exchange Relation and the Origin of Planetary Rotation

7.1 Location Adaptability of Exchange Demand

According to the element–environment relation, environmental matter–energy density ρ increases as heliocentric distance rr decreases. The high-ρ near-Sun region should therefore be more favorable for planets that maintain a large exchange quantity J, corresponding to large mass. Observations show the opposite: the near-Sun region (Mercury to Mars) contains small-mass planets, while the far-Sun region (Jupiter to Neptune) contains large-mass planets [2]. This raises a core adaptability question. Within exchange mechanics, how do small-mass planets avoid excess exchange demand in high-ρ environments? How do large-mass planets overcome insufficient exchange demand in low-ρ environments?

7.2 Observed Correlation Between Rotation Speed and Mass

Table 3 Observed correlation between rotation and mass of the eight planets (data source: [2]; m/Tm/T is the ratio relative to Jupiter)

Planet	**Mass (Earth = 1)**	**Rotation period T**	**m/T (relative value)**
Jupiter	317.94	9.86 h	0.5389
Saturn	95.18	10.23 h	0.1550
Neptune	17.22	16.11 h	0.0159
Uranus	14.63	16.80 h	0.0152
Earth	1.00	23.93 h	0.000696
Venus	0.82	5832 h	0.00000234
Mars	0.11	24.62 h	0.0000745
Mercury	0.05	1407.6 h	0.000000595

Table 3 shows that the m/T sequence for Jupiter, Saturn, Neptune, Uranus, Earth, and Mercury matches the descending order of mass mm. Only Venus and Mars deviate, but their m/T values do not exceed the descending range of adjacent-mass Earth and Mercury, so Venus and Mars also largely follow this regularity; other factors cause some deviation. Those factors are a research direction and are not discussed here. On the basis of this observed correlation, we adopt the following empirical limiting relation:

$$m \propto v_{\text{rot}} \qquad (7.1)$$

Note. Eq. (7.1) is a symbolic expression of a trend empirical correlation, not a dimensionally strict quantitative formula. Observations suggest that the mass mm of the eight planets is positively correlated in trend with rotational linear velocity v_{rot}. The quantitative form of Eq. (7.1) is a direction for future work.

The derivation of Eq. (7.1) contains a logical leap: the proportional relation between planetary mass mm and intrinsic exchange quantity J ($m \propto J$) has not been rigorously demonstrated. In the present version, Eq. (7.1) is introduced as an empirical relation, and its theoretical basis is a direction for future work. It follows that

$$J \propto v_{\text{rot}} \qquad (7.2)$$

Note. As with Eq. (4.1), Eq. (7.2) is a symbolic expression of a trend empirical correlation. Its quantitative form is a direction for future work.

7.3 Establishment and Physical Interpretation of the Environmental Exchange Relation

(1) Form of the relation

Combining the element–environment relation $J \propto \rho$ with the observed relation in Eq. (7.2) yields a basic equation linking planetary intrinsic properties, motion state, and environmental parameters—the environmental exchange relation:

$$J \propto v_{\text{rot}} \cdot \rho\big|_{\uparrow\downarrow} \qquad (7.3)$$

Note. Eq. (7.3) combines Eqs. (4.1) and (7.2) and is likewise a symbolic form of a trend empirical correlation. The symbol "$|_{\uparrow\downarrow}$" indicates that ρ and v_{rot} must vary inversely.

(2) Physical meaning: product relation and resolution of the exchange contradiction

In reality, $J \propto \rho$ and $J \propto v_{\text{rot}}$ hold simultaneously, which creates an exchange contradiction: if both hold simultaneously, then ρ and v_{rot} must be proportional; observations show instead that they are inversely proportional.

The exchange relation $J \propto v_{\text{rot}} \cdot \rho|_{\uparrow\downarrow}$ is proposed to resolve this contradiction. It is not a simple combination of two independent proportional relations; it states that J is the product of v_{rot} and ρ. J is jointly determined by rotational linear velocity v_{rot} and environmental density ρ, and their contributions to J are multiplicative.

(3) Key corollary: when J is fixed, $\mathbf{v_{rot}}$ and ρ are inversely proportional

From Eq. (7.3),

$$v_{\text{rot}} = \frac{J}{\rho} \quad or \quad \rho = \frac{J}{v_{\text{rot}}} \tag{7.4}$$

The larger the environmental density ρ, the smaller the rotational linear velocity v_{rot} must be; the smaller ρ, the larger v_{rot} must be. When J is fixed, ρ and v_{rot} must vary inversely. The observational fact that ρ and v_{rot} are inversely proportional is therefore not a contradiction but an inevitable result under J conservation.

(4) Note on the proportionality constant

Two types of force action should be distinguished.

Determinative forces, such as universal gravitation, adopt a fixed proportionality constant k, such as $G = 6.674 \times 10^{-11} N \cdot m^2/kg^2$, because their magnitude is definite and calculable.

Auxiliary forces, such as the exchange force and thrust discussed here, should not adopt a fixed proportionality constant; a same-direction proportional trend is sufficient. If two quantities are both proportional to a third, their proportionality coefficients may differ, for example 8 and 1.2, but both must be positive. If one is positive and the other negative, they do not constitute a same-direction trend.

The environmental exchange relation belongs to auxiliary force action, so we use a symbolic expression of proportional trend (\propto∝) and do not introduce a fixed proportionality constant.

(5) Explanation of observational facts

Eq. (7.4) offers a possible physical explanation for the rotation differences among Solar System planets:

Jupiter and Saturn (low-ρ region): low environmental density; to maintain the same J, high v_{rot} must compensate, explaining the rapid rotation of giant planets;

Mercury and Venus (high-ρ region): high environmental density; to maintain the same J, low v_{rot} must avoid excessive exchange, explaining the slow rotation of terrestrial planets;

Earth (intermediate-ρ region): intermediate environmental density, with intermediate rotation speed.

(6) Relation to the adaptability question

The adaptability question in Section 7.1—how small-mass planets avoid excess exchange in high-ρ regions, and how large-mass planets overcome insufficient exchange in low-ρ regions—is answered by Eq. (7.4):

Large-mass planets (large J) in low-ρ regions: large J requires large $v_{\text{rot}} \cdot \rho$; if ρ is small, v_{rot} must be large;

Small-mass planets (small J) in high-ρ regions: small J requires small $v_{\text{rot}} \cdot \rho$; if ρ is large, v_{rot} must be small.

7.4 Alternating Bipolar Inlet–Outlet Structure

7.4.1 Limitations of a Fixed Bipolar Structure

In a fixed bipolar inlet–outlet structure, the front side is permanently an inlet region and the back side is permanently an outlet region. The disadvantage is that the matter–energy exchange flow must be transported across the entire body diameter ($2R$). The longer the path, the greater the energy dissipation from internal resistance. As body radius R increases, this dissipation grows linearly, severely limiting the maximum exchange flux the body can maintain.

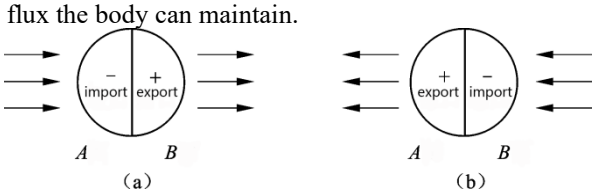


Fig. 5 Schematic of an alternating bipolar inlet–outlet structure.

(a) At time tt: region A is inlet, region B is outlet. (b) At time $t + T/2$: region A switches to outlet, region B switches to inlet.

7.4.2 Definition, Formation, and Advantages of the Alternating Structure

To overcome the dissipation bottleneck of the fixed structure, large celestial bodies evolve an alternating bipolar inlet–outlet structure. Through rotation, the same physical region on the body's surface periodically switches between inlet and outlet functional states (Fig. 5).

The alternating structure has clear advantages over the fixed structure:

(1) Shortened path, halved dissipation. The effective transport path of the exchange flow is shortened from the diameter $2R$ to the radius R.

(2) Improved efficiency. The inlet and outlet functions can switch frequency as needed.

(3) Full-surface participation. The entire spherical surface periodically undertakes inlet and outlet functions.

7.4.3 Regulation Mechanism of Rotation Frequency

Rotation is essentially the means by which the alternating structure achieves efficient exchange. Just as organisms regulate breathing frequency to match metabolic rate, celestial bodies regulate their rotational angular velocity ω, or frequency $f = \omega/2\pi$, to match their exchange demand J:

$$J \propto f \qquad (7.5)$$

Combined with the environmental exchange relation (7.3), under a given environmental density ρ, a celestial body adjusts its rotation frequency f so that its effective exchange quantity J reaches equilibrium with the environment.

7.4.4 Multi-Scale Unified Role of the Celestial Body Inlet–Outlet Structure

The alternating inlet–outlet structure provides a dynamical framework that unifies internal physics, surface geology, orbital motion, and rotation of celestial bodies.

(1) As an exchange channel. It is the basic functional unit for bidirectional matter–energy exchange between the celestial body and the interstellar medium, solar wind, and other external media.

(2) Control of geological structure. The type of inlet–outlet structure (fixed or alternating) and its spatial distribution may influence the crust–mantle structure, topographic differentiation, and direction of material migration of celestial bodies. This corollary is discussed in detail in earlier studies [9,10] and is not expanded here.

(3) Unified driving and modulation of revolution and rotation.

Revolution modulation. When Earth is regarded as a fixed bipolar inlet–outlet structure, the net flow force difference arises from absorption and release of solar exchange flow by the dayside and nightside hemispheres. This is the physical essence of the thrust formula (5.12).

Rotation regulation. When Earth is regarded as an alternating bipolar inlet–outlet structure, rotation is an adaptive behavior that reduces exchange dissipation and regulates exchange quantity J through frequency f to adapt to the environment ρ.

The revolution modulation mechanism has been demonstrated in detail in this paper. The corollary of geological structure control is currently hypothetical and requires further testing in future observations of celestial body internal dynamics and geology.

8 Applications to Solar System Sub-Regions

8.1 Dynamical Origin of the Asteroid Belt and Planetary Rings

8.1.1 Comparison Between the Kuiper Belt and the Main Asteroid Belt

The Kuiper Belt and the main asteroid belt are products of the specific evolutionary stage of a dispersed asteroid belt in the low- and intermediate-velocity zones, respectively.

(1) Kuiper Belt (low-velocity zone). Its front end connects with the diffuse Oort Cloud, and its back end transitions to condensed bodies such as Neptune. Sheltered by the weak solar radiation environment, its total mass is large, and it contains many large bodies with radii of the order of a thousand kilometers, such as Eris [17].

(2) Main asteroid belt (intermediate-velocity zone). Its front end connects with the Trojan group of Jupiter's orbit (diffuse state), and its back end points to the condensed Mars. Because solar radiation action is stronger in the intermediate-velocity zone, it cannot maintain a massive, loose material collection like the Kuiper Belt.

8.1.2 Evolutionary Connection Between the Trojan Group and the Main Asteroid Belt

The Trojan group can be regarded as the primary diffuse form of material evolution in the intermediate-velocity zone, sharing an orbit with Jupiter and exhibiting a mixed state. The main asteroid belt is its advanced semi-aggregated form.

8.1.3 Dynamical Interpretation of Planetary Rings and Cometary Orbits

(1) Origin of planetary rings. Jovian planets lie in the low-velocity zone, where solar radiation action is weak. Small bodies of light substances such as dust and ice particles receive weak solar net thrust there, so they can stably reside under the gravitational action of Jovian planets and form planetary ring systems. Terrestrial planets, by contrast, lie in the intermediate- and high-velocity zones, where solar radiation action is strong. Tiny light-material particles receive relatively strong solar net thrust and cannot stably exist around terrestrial planets, so terrestrial planets do not form planetary rings.

(2) High-eccentricity cometary orbits. Comets are essentially aggregates of light elements such as ice and dust, with small exchange demand JJ, and should originally exist in the far-Sun low-velocity zone. However, the release force F_{out} of comets, especially when active, is relatively large. According to the thrust formula, a larger net thrust drives them to migrate inward into the Solar System. The contrast between the two produces strong oscillation and high-eccentricity orbits.

8.2 Thrust Effects on Tiny Bodies

Tiny bodies in the far-Sun region (Kuiper Belt objects, comets, dust) have no significant internal heat ($P_{\text{int}} \approx 0$), but the side facing the Sun can still be regarded as an inlet and the side facing away as an outlet. Although the magnitude is small, thrust still exists, and its direction is set by the day–night temperature difference. This mechanism allows the thrust formula to explain why airless bodies such as diffuse states, asteroids, and comets also show radial gradation trends similar to those of planets.

8.3 Limitations of Conceptual Operationalization and Future Work

The exchange mechanics framework proposed here involves several core concepts that have not yet been fully operationalized. Their quantification is an important direction for future work. To avoid misunderstanding, they are summarized here.

(1) Quantification of exchange quantity J. J is defined here as an intrinsic property of elements; its numerical value, dimension, and relation to known physical quantities have not yet been established. Relations such as $J \propto \rho$ (Eq. 4.1) and $J \propto v_{\text{rot}}$ (Eq. 7.2) should be understood as trend empirical correlations, not strictly quantitative formulas. Quantifying J requires coordinated progress in first-principles atomic physics, interstellar molecular spectral line analysis, and numerical simulation.

(2) Operational definition of environmental density ρ. Whether ρ should include energy density, and whether the total mass density of the interplanetary medium should be used, remain to be determined.

(3) Empirical nature of the three-zone boundaries. The boundaries (5.2 AU, 1 AU) are empirical divisions (Chapter 2), and their theoretical basis requires further work.

(4) Applicable stage of the thrust formula. The quantitative effect of the thrust formula may be significant during the early planetesimal stage ($F_{\text{net}}/F_{\text{grav}} \approx 10^{-2} - 10^{0}$), but is only a minor modulation during the current planetary stage ($F_{\text{net}}/F_{\text{grav}} \approx 10^{-15}$) (Section 5.8). This paper does not claim that the thrust formula can explain the current macroscopic configuration of planets; it positions the formula as a candidate mechanism for the early planetesimal aggregation stage.

(5) Influence of the inlet–outlet structure on geological structure. Section 7.4.4 notes that the inlet–outlet structure may influence the crust–mantle structure and topographic differentiation of celestial bodies; this corollary is currently hypothetical. One case deserves particular attention. When the Sun is regarded as a release source, Earth can be regarded as a fixed bipolar inlet–outlet structure. When Earth is regarded as a release source, the Moon can also be regarded as a fixed bipolar inlet–outlet structure: the Moon's near side faces Earth and its far side faces away. Whether these two cases are necessarily connected provides an excellent test of inlet–outlet theory.

These limitations do not affect the core contributions of the paper. The geometric derivation of the thrust formula (Sections 5.2–5.4) is rigorous; the empirical pattern of three-zone gradation (Chapter 2) summarizes observational facts; and the falsification paths (Chapter 9) are explicit. This paper proposes a theoretical framework; it does not present an established quantitative theory.

9 Falsifiability

(1) Three-zone division. If piecewise fitting of a larger sample (including exoplanets) places the slope change points of the radius–heliocentric distance relation away from Jupiter's orbit (5.2 AU) and Earth's orbit (1 AU), the division needs revision.

Prediction: For confirmed exoplanetary systems, normalized slope change points should lie near $r/r_{\text{Jupiter}} \approx 1$ and $r/r_{\text{Earth}} \approx 1$.

Threshold: If the normalized distances fall outside 0.8–1.2, the division needs revision.

Source: NASA Exoplanet Archive.

(2) Thrust formula. If Jupiter's and Saturn's nightside internal heat radiation flux is similar to the dayside (after subtracting reflected sunlight), the formula needs revision.

Prediction: The thermal flux ratio should satisfy $T_{\text{night}}/T_{\text{day}} > 1$ (nightside hotter).

Threshold: If $T_{\text{night}}/T_{\text{day}} < 1.05$, the formula needs revision.

Source: JWST NIRSpec observations of Jupiter's nightside (5–28 μm).

(3) Element–environment relation. A body system dominated by high-J elements in a low-ρ environment, unexplainable by other mechanisms, would require revising or abandoning $J \propto \rho$.

Test: High-sensitivity spectral observations of low-ρ environments (interstellar molecular clouds, planetary nebulae), measuring heavy-element molecule abundances against the trend predicted by $J \propto \rho$.

(4) Environmental exchange relation. If exoplanet observations show a systematic contradiction between rotation rate, mass, and environmental density and the prediction of $J \propto v_{\text{rot}} \cdot \rho$, the relation needs revision. Because J lacks a definite dimension, "prediction" here means trend direction, not quantitative value.

Test: For exoplanets with measured rotation rates, test the correlation between $v_{\text{rot}} \cdot \rho$ and m.

(5) Earth–Moon geological similarity. Earth and the Moon appear to share an exchange division of labor (Arctic Ocean inlet–Antarctica outlet for Earth; near side inlet–far side outlet for the Moon). If no such division exists, inlet–outlet theory needs revision.

Test: More detailed comparative analysis of Earth–Moon geological structures. High-precision topographic measurements of non-tidally locked planets (Jupiter, Saturn) to check for systematic dayside–nightside concave–convex differences.

10 Compatibility

Newtonian gravity. The thrust formula and gravitational formula are kinematically compatible (Section 5.9). Thrust does not replace gravity; it offers a complementary radial-modulation perspective.

Temperature gradient model. $J \propto \rho$ does not contradict this model. Differences in J affect condensation and accretion efficiency across environments [15,6].

Standard planet formation. The bipolar inlet–outlet structure follows naturally from day–night asymmetry. Standard theory (Chambers 2004 [5]; Raymond et al. 2009 [6]) explains accretion and compositional differentiation. Our framework adds an explanation for the non-monotonic radius–distance relation.

Nice and Grand Tack models. The Nice model (Tsiganis et al. 2005 [3]) explains giant-planet orbital migration; Grand Tack (Walsh et al. 2011 [4]) explains Mars's small mass. Our framework explains the radius–density–rotation gradation. The levels differ and can complement each other.

Standard theory already explains compositional differences (temperature gradient), orbital migration, Mars's mass, and the overall rotation trend (angular momentum conservation). Our distinctive contribution is a possible mechanism for the non-monotonic radius–distance relation and an attempt to place revolution and rotation in one framework. Whether these contributions are necessary should be assessed by future comparative work.

11 Conclusions

1. A net thrust model of orbital motion. By treating a body as a bipolar inlet–outlet structure, we derive from electromagnetic momentum flux:

$$F_{\text{net}} = \frac{2\pi R^2}{3c}\left(\varepsilon_{\text{day}}\sigma T_{\text{day}}^4 - \varepsilon_{\text{night}}\sigma T_{\text{night}}^4\right) + \frac{\pi R^2 F_{\odot} A}{c}\backslash k$$

The formula distinguishes sphere (zero net force) from hemisphere (non-zero), and argues for the microscopic homology of solar, planetary, and atomic radiation. The model suggests orbital behavior may be modulated by dayside–nightside radiation balance. The thrust is a modulating force, not a driving force; gravity dominates revolution kinematics, thrust modulates radial equilibrium (Section 5.9).

2. Applicable stage. During the early planetesimal stage ($F_{\text{net}}/F_{\text{grav}} \approx 10^{-2} - 10^{0}$), thrust may have substantially influenced radial distribution. This is the main applicable stage for Chapter 6.

3. Three-zone gradation as a test case. From the eight planets, we identify the non-monotonic radius–distance pattern. The three-zone division motivated the formula; the formula offers a possible physical explanation for the trend reversal. Critical heliocentric distances require future work.

4. Environmental exchange relation. $J \propto v_{\text{rot}} \cdot \rho|_{\uparrow\downarrow}$ is proposed as a working hypothesis. The relation suggests J may be jointly modulated by rotation velocity and environmental density; "$|_{\uparrow\downarrow}$" means that when J is fixed, the two vary inversely.

5. Alternating inlet–outlet structure and rotation. To overcome path dissipation in the fixed structure, large bodies evolve an alternating bipolar structure, realized through rotation.

6. A possible unified framework. This paper attempts to place revolution, rotation, scale sequence, internal structure, and system distribution under one perspective. The framework is at the proposal stage: the thrust effect may be significant early but only a minor modulation now; the exchange relation is not yet observationally supported; three-zone boundaries are empirical. "Unified dynamical interpretation" is a goal, not a result. Future numerical work and systematic observational tests should evaluate its necessity and explanatory power.

Positioning. The thrust formula, inlet–outlet theory, and element–environment relation are at the framework-proposal stage. The thrust formula's scope is limited to the early planetesimal stage and to current small bodies with significant internal heat. Falsification paths are in Chapter 9. Quantitative testing requires JWST observations of Jupiter's and Saturn's nightside internal heat radiation, and systematic exoplanet rotation and environmental density measurements.

Compliance with Ethical Standards:

Funding: Not applicable.

Conflict of Interest: All authors disclosed no relevant relationships.

Author contributions: All authors contributed equally.

Data Availability: Not Applicable.

Ethics approval and Consent to participate: Not applicable.

Acknowledgments: Not applicable.

References

[1] Newton I. Philosophiæ Naturalis Principia Mathematica[M]. London: Royal Society, 1687.
[2] NASA Planetary Fact Sheet [DB/OL]. NASA Goddard Space Flight Center, 2023. https://nssdc.gsfc.nasa.gov/planetary/factsheet/
[3] Tsiganis K, Gomes R, Morbidelli A, Levison H F. Origin of the orbital architecture of the giant planets of the Solar System[J]. Nature, 2005, 435(7041): 459–461.
[4] Walsh K J, Morbidelli A, Raymond S N, O'Brien D P, Mandell A M. A low mass for Mars from Jupiter's early gas-driven migration[J]. Nature, 2011, 475(7355): 206–209.
[5] Chambers J E. Planetary accretion in the inner Solar System[J]. Earth and Planetary Science Letters, 2004, 223(3–4): 241–252.
[6] Raymond S N, O'Brien D P, Morbidelli A, Kaib N A. Building the terrestrial planets: Constrained accretion in the inner Solar System[J]. Icarus, 2009, 203(2): 644–662.
[7] Zhao D Y, Liu S N. Fundamentals and Applications of Exchange Equilibrium Mechanics[M]. Changsha: Central South University Press, 2004. (in Chinese)
[8] Zhao D Y, Liu S N. Relationship between geological gradation motion and existing environment of the Solar System[J]. Acta Geologica Sichuan, 2022, 42(152): 556–563. (in Chinese)
[9] Zhao D Y, Liu S N. Introduction to the "inlet–outlet" geological structure of the Earth–Moon system[J]. Acta Geologica Sichuan, 2023, 43(153): 22–31. (in Chinese)
[10] Zhao D Y, Liu S N. Viewing the geological gradation laws of the Solar System from the action of inlet–outlet geological structural forces[J]. Acta Geologica Sichuan, 2023, 43(154): 202–211. (in Chinese)
[11] Bottke W F, Vokrouhlický D, Rubincam D P, Nesvorný D. The Yarkovsky and YORP effects: Implications for asteroid dynamics[J]. Annual Review of Earth and Planetary Sciences, 2006, 34: 157–191.
[12] Snow T P, McCall B J. Diffuse Atomic and Molecular Clouds[J]. Annual Review of Astronomy and Astrophysics, 2006, 44: 367–414.
[13] Bian D P. The Mysterious Starry Sky[M]. Beijing: Science Popularization Press, 1988. (in Chinese)
[14] McGuire B A. 2021 Census of Interstellar, Circumstellar, Extragalactic, Protoplanetary Disk, and Exoplanetary Molecules[J]. The Astrophysical Journal Supplement Series, 2022, 259(2): 30.
[15] McSween H Y, Huss G R. Cosmochemistry[M]. Cambridge: Cambridge University Press, 2010.
[16] Hevey P J, Sanders I S. A model for planetesimal meltdown by 26Al and its implications for meteorite parent bodies[J]. Meteoritics & Planetary Science, 2006, 41(1): 95–106.
[17] Morbidelli A, Brown M E, Levison H F. The Kuiper Belt and the Primordial Evolution of the Solar System[M] // Festou M C, Keller H U, Weaver H A (eds). Comets II. Tucson: University of Arizona Press, 2004: 275–292.
[18] Guillot T. Interiors of Giant Planets Inside and Outside the Solar System[J]. Science, 1999, 286(5437): 72–77.
[19] Einstein A. Erklärung der Perihelbewegung des Merkur aus der allgemeinen Relativitätstheorie[J]. Sitzungsberichte der Königlich Preußischen Akademie der Wissenschaften, 1915: 831–839.